20th Australasian Fluid Mechanics Conference
Perth, Australia
5-8 December 2016

A Study on the Flow Field and Internal Circulation of a Single Moving Droplet

E. Mohammadi, A. King and R. Narayanaswamy

Fluid Dynamics Research Group, Department of Mechanical Engineering
Curtin University, Western Australia 6102, Australia

Abstract

A single water droplet is considered to be moving in a confined chamber filled with paraffin oil. The droplet diameter is 2 mm and the chamber dimension is 1 cm $\times$ 1 cm $\times$ 1 cm. Multiphase VOF solver of OpenFOAM CFD code is utilized to do the numerical study to ascertain the inner flow field of the droplet in terms of the swirling strength and velocity components of the droplet. An appropriate geometrical component (baffle) is positioned in the chamber to investigate the effect of ambient flow field condition on the internal flow of a droplet. This study is part of a wider research investigating the impact of ambient turbulent flow field on the internal circulation of a droplet, and the consequence on evaporation rate of spray in different applications such as spray cooling, diesel engines and gas turbines.

Introduction

The study of flow field inside a droplet provides information on improving spray efficiency from spray cooling, combustion in gas turbines and diesel engines, the spraying of pesticides for land-based vegetation as well as knowledge of the transport of rain drops. In early studies specifically the circulation pattern inside the droplet was the subject of some papers, e.g. Spells [11], Garner and Skelland [5] and Megaridis et.al. [8]. The relative viscosity between the droplet fluid and the ambient fluid generates shear stress on the interface of the droplet; internal circulation of the fluid within the droplet results as a consequence of this shear stress. The effect of internal circulation on the mass transfer of the droplet was the subject of few other published work. Burkhart, et.al.[2] studied cases with no circulation to full circulation pattern inside a droplet during the formation of the droplet and evaluated the variation of mass transfer. Vaporization of droplet by considering internal temperature distribution due to internal motion is analysed by Prakash and Sirignano [9]. The convection inside the droplet is demonstrated by a parameter known as the swirling strength. The influence of mass on the swirling strength is discussed in Wang et.al.[13]. The velocity flow field inside the droplet has been studied in [6]. In high-speed atomizing sprays, the transfer of momentum between drops and gas phase causes the deformation and sometimes breakup of the drops. It is also shown that the deformation of drops are affected by the drag coefficient (Liu et.al.[7]). Transient deformation and change of drag coefficient of a droplet has been elucidated in ([10] and [12]).

To answer the question if outside turbulent flow field changes the internal circulation of a droplet, i.e., how outside flow field affects the interior flow field of a droplet, increases circulation and mixing to improve heat transfer heads us to study the flow field inside a droplet when it is freely falling. Asymmetrical outside flow field is imposed to emphasise the effect of external condition to the internal circulation and the intensity as well.

Model Description and Numerical Models

Due to similar studies and for validation of the case, a spherical water droplet with 2 mm diameter freely falling in a confined chamber with dimension of 1 cm $\times$ 1 cm $\times$ 1 cm filled with paraffin oil is considered (Figure 1). A baffle 1 mm in height (in y direction) and 3 mm in width (in x direction) is placed to impose asymmetry state into flow field. As baffle in z direction has full length (1 cm) it provides axi-symmetrical geometry and allow comparison in axi-symmetrical and asymmetrical condition. To have enough refined mesh and also save computational time, dynamic mesh refinement technique is used. The refined mesh area moves down when droplet falls down. The number of volumetric cells in 0 time while no refinement starts are 121250, but as soon as simulation starts, it increases to nearly 4 times. However, the exact number of cells in each time step varies according to the condition of flow. To prevent from the spurious currents in two-phase interface the proper time step according to minimum mesh size is used [4]. Figure 2 shows the case setup during simulation. The refined mesh zone around the droplet and the baffle are shown. For solving the incompressible Navier-Stokes equation VOF (Volume Of Fluid) approach based on interface capturing method is employed. OpenFOAM, an open source numerical software for executing the numerical study is used. Since temperature variations are not considered in this work energy equation is not solved. Unsteady first order Euler method for time discretization and second order discretization methods for space are utilized. The pressure-velocity coupling is attained by PIMPLE method which is the combined form of Pressure Implicit Split Operator (PISO) algorithm and Semi Implicit Method for Pressure Linked Equation (SIMPLE) algorithm. In PIMPLE, the PISO algorithm as well as relaxation factors of SIMPLE are employed. All boundaries are set as wall, except the top boundary, which is considered as atmospheric boundary condition.

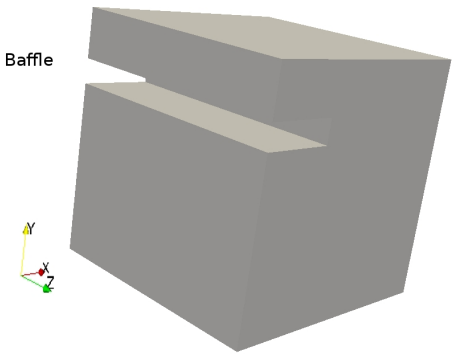

Figure 1: Geometrical domain

For the validation of the numerical model, the terminal velocity of the droplet obtained using the modelling approach is compared with the theoretical model of Stokes, applicable for a rigid sphere, small bubbles and droplets [3]. The validation is done without considering the effect of the baffle inside the chamber to be comparable to the theoretical model. Figure 3 shows the falling velocity of the drop during the time and the theoretical

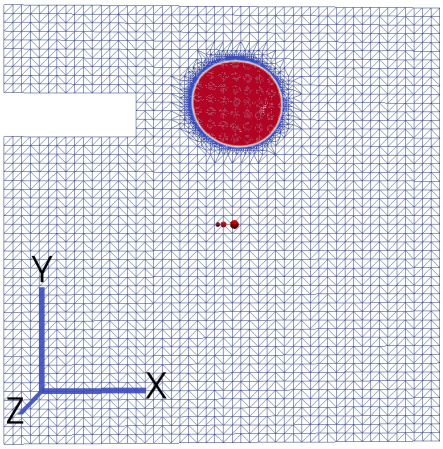

Figure 2: Case setup

terminal velocity based on Stoke's law as well. As seen from figure 3, the terminal velocity of the droplet obtained from the present work is in good agreement with the theoretical model, having a 6% difference which emphasises the accuracy of the numerical settings in the present work.

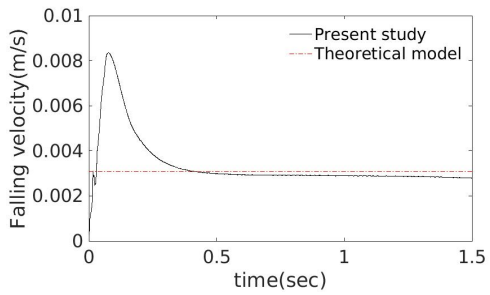

Figure 3: Numerical and theoretical terminal velocity comparison

Another validation has been shown in Figure 4 which shows the stream lines inside the droplet in a symmetrical flow field, i.e., no baffle. As shown in figure 4 the two big vortices of Hadamards theoretical vortices inside a droplet [11](figure 5) are obvious in the current study.

Results and Discussion

Figure 6 illustrates the stream lines inside and around the droplet in the middle plane of the droplet in the xy surface at 0.3 sec. The middle plane of the droplet is where the maximum swirling strength happens. The presence of vortices is due to the relative viscosity between two fluids that causes shear stress at the interface and then continues to migrate the interior of the droplet. However, the two vortices are asymmetrical unlike seen in figure 4. This is due to the consequence of the presence of a non-symmetrical flow field created by a baffle inside the chamber. Additionally, some small vortices mainly near the interface can also be seen. Hence, to quantify rotation and shear stress in the flow field, swirling strength is used which shows the power of local vortices [1] and convection effects [13]. For velocity vector $\mathbf{V} = u\hat{i} + v\hat{j} + w\hat{k}$ the gradient of velocity vector is

$$\mathbf{J} = \nabla\mathbf{V} = \begin{bmatrix} \partial u/\partial x & \partial u/\partial y & \partial u/\partial z \\ \partial v/\partial x & \partial v/\partial y & \partial v/\partial z \\ \partial w/\partial x & \partial w/\partial y & \partial w/\partial z \end{bmatrix} \quad (1)$$

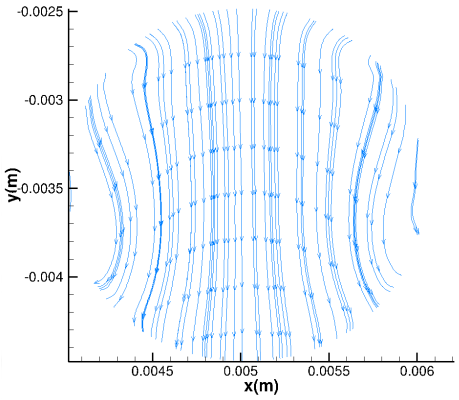

Figure 4: Velocity vectors inside the droplet in symmetrical chamber

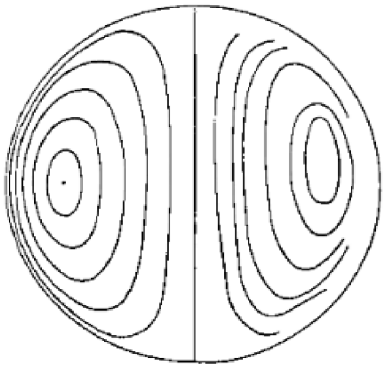

Figure 5: Hadamard's vortices inside droplet[11]

Eigenvalue of $\mathbf{J}$ is identified by solving the following equation:

$$det(\mathbf{J} - \lambda\mathbf{I}) = 0 \quad (2)$$

Where λ is the eigenvalue, and $\mathbf{I}$ is the identity matrix. For the above cube equation if the discriminant of characteristic equation is negative, the equation has three roots; a real one, λ_r, and two complex conjugates, $\lambda_{cr} + i\lambda_{ci}$ and that $\lambda_{ci} > 0$ shows the strength of local vortices which is the swirling strength. Figure 7 depicts swirling strength in the flow field shown in figure 6.

As λ_{ci}^{-1} demonstrates the period of rotation around λ_r axis, for big vortices that the period of rotation is infinitive, $\lambda_{ci}^{-1} = 0$. Therefore, swirling strength displays areas that have local small vortices corresponding to $\lambda_{ci} > 0$. But for areas that swirling strength is zero, it does not interpret to no local vortex. As a result, in figure 7 the areas near the big vortices, corresponding to the G and the H regions, swirling strength is zero. Nevertheless, the swirling strength contour still reveals lot of useful information about the local small vortices near the interface. For example, the highest swirling strengths are located in the interface, corresponding to the A to the F regions, that tolerates shear stress of difference between two moving fluids. Swirling strength contour also exhibits the non symmetrical flow field inside the droplet. It can be deduced by comparing figure 4 where the flow field is symmetrical and figure 6 that the flow field is asymmetrical. Comparing swirling strength in the xy plane that experiences the highest swirling strength (figure 7) with

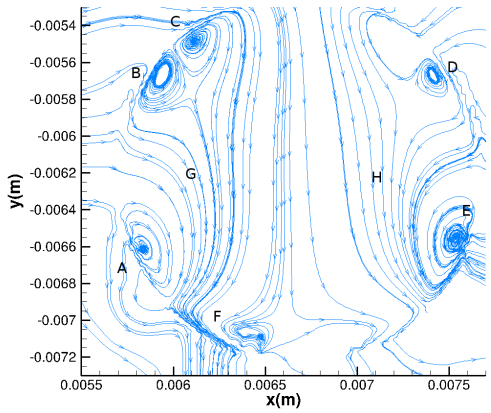

Figure 6: Velocity vector field inside and around the droplet in asymmetrical chamber (present work)

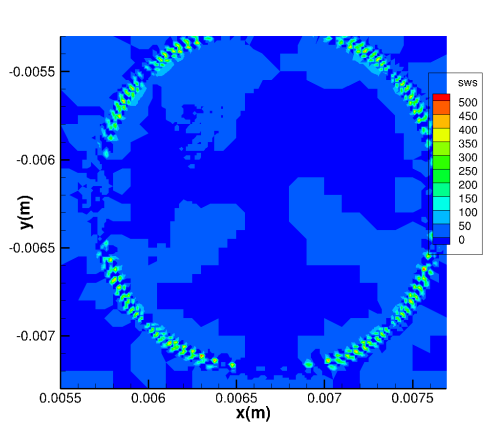

Figure 7: Swirling strength inside and around the droplet

the swirling strength of the zy plane with the highest swirling strength (figure 8) is another evidence for the effect of symmetrical and non symmetrical outer flow field. As it can be seen the swirling strength in the zy plane of the droplet is nearly symmetrical. On the other hand, the swirling strength in the xy plane is quite asymmetrical and shows the influence of baffle.

Another aspect of droplet flow field is revealed by looking at figure 9 which shows average velocity components of the droplet while there is a baffle inside the chamber. The baffle causes the droplet not to get to stable condition, terminal velocity, yet (comparing with symmetrical case, i.e., figure 3). Although there is no external force in the x direction, the x component of velocity, u, varies in time especially at the very first steps of falling where the droplet is nearer to the baffle. Importantly, the maximum value of the u is higher than the maximum value of the v for the very first time steps. Meanwhile, no meaningful variation during the time for the w, the z component of velocity is observed because of axisymmetrical structure of the baffle about the z axis.

Looking at the inside flow field of the droplet helps to have deeper view of physical phenomena around the droplet. Figure 10a, 10b and 10c show vertical velocity contours inside the droplet in the plane perpendicular to z-axis at the centre of the drop at time steps with great velocity changes according to

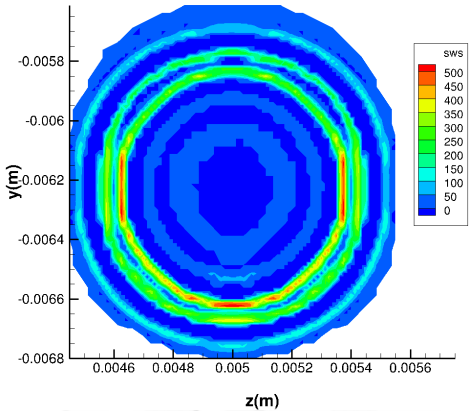

Figure 8: Swirling strength inside and around the droplet in the zy plane of the droplet

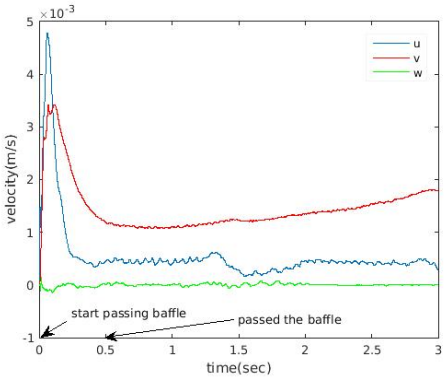

Figure 9: Average drop velocity components

figure 9, i.e 0.13, 0.30 and 0.48 seconds, respectively. Considering figure 10a, the y component of velocity has negative values in a major part in the middle of the droplet where the maximum values are at the lower half of the drop. Negative direction represents the falling direction. Although, there are small areas with positive velocity values, mostly near lateral interface. That shows circulation in this region. At 0.30 second the major change in the y component of velocity contour happens in maximum value of negative velocity which drops to about -0.00316 m/s from -0.002 m/s. Although, there is a small area with -0.00316 m/s values at 0.13 sec but comparing to the case of 0.30 sec is negligible. The areas with upward velocity and zero velocity still have nearly the same condition. Later in 0.48 second the y component of velocity speeds up in the whole middle of the drop. However, the areas with maximum upward velocity near the interface feel no noticeable change. So the majority of areas in droplet have vertical velocity in downward direction. This emphasise that the y component of velocity is less affected by outside flow field.

Figure 10d, 10e and 10f depict the x component of velocity contours in the x middle plane of drop at 0.13, 0.30 and 0.48 seconds, respectively. Magnitude of the x-velocity at 0.13 second is mainly positive with highest value of 0.00227 m/s. The positive value of velocity is the direction opposite of the baffle. At 0.30 second, area with zero velocity grows and covers bigger space. At 0.48 second most of the areas have negative value or zero values for the x component of velocity that shows that the velocity vector direction turns during this period of time. Due to the

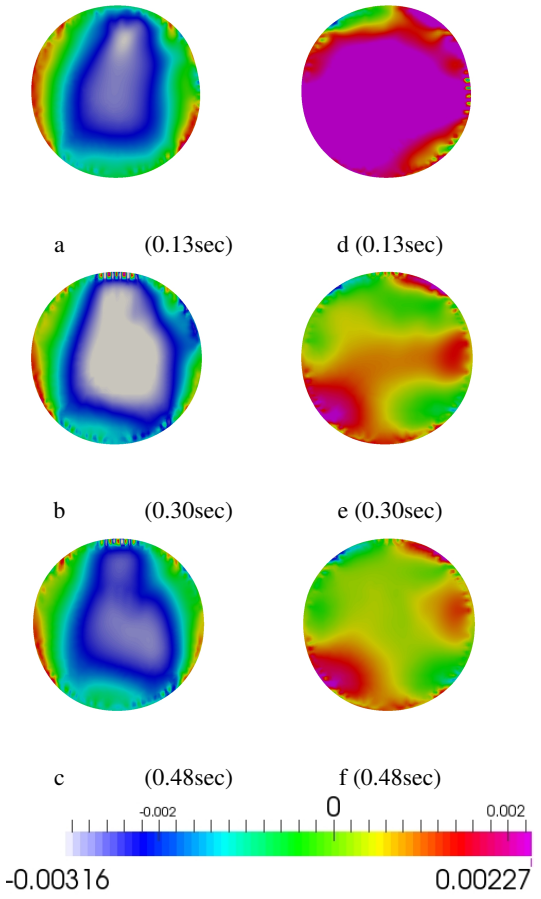

Figure 10: Contour of y component of velocity a, b, and c. Contour of x component of velocity d, e and f.

change of the x-component and small y-component variation, especially in the middle areas, the presence of elliptical shapes of vortices in the middle of the drop is confirmed. Additionally, the x-component is affected by the outer flow field more than the y-component of velocity. The reason might be that gravity in the y direction is more prominent than shear stress that is not able to alter the y-velocity in a majority of the regions.

In conclusion, although the y component of velocity feels some changes, the major variation tolerates by the x component of velocity. This will help enhance mixing within the droplet.

Conclusions

The internal flow field inside a single droplet is studied by considering swirling strength and velocity components when it is falling freely. The comparison of terminal velocity of the droplet with a theoretical relation and stream lines pattern inside the droplet with a theoretical model show good agreement. The swirling strength parameter is able to show local small vortices inside the droplet. An asymmetrical baffle, in the xy plane, inside the chamber causes asymmetrical flow field in the droplet that can be seen in the x component of the velocity and the swirling strength as well. On the other hand, nearly zero values for the z component of the velocity and symmetrical behaviour during the time strengthen the fact that, the change in the ambient condition leads the variation in the internal flow of the drop. Particularly, comparison the swirling strength contour in the x middle and the z middle planes completely agrees with this idea. Furthermore, the non-zero values for the x component of the velocity is the evidence of circulation and shear stress in the interior of the droplet that emphasises mixing. As the existence of gravity in the y direction prevents the y-component of velocity to change as much as the x-component; this question is arisen that if there is a bigger force in the x-direction to encounter gravity if the changes and consequently the circulation and the mixing would be greater. Undoubtedly, increase of mixing is a pleasant phenomena in heat transfer leading to better evaporation and enhanced spray efficiency which is the ultimate purpose of our research.

References

[1] Adrian, J.R., Christensen, T.K. and Liu, Z.C., Analysis and Interpretation of Instantaneous Turbulent Velocity Fields, *Experiments in Fluids*, **29**, 2000, 275–290.

[2] Burkhart, L., Weathers, P.W. and Sharer, P.C., Mass Transfer and Internal Circulation in Forming Drops *AIChE Journal*,**22**, 1976, 1090–1096.

[3] Clift, R., Grace, J. R. and Weber, M. E., *Bubbles, Drops, and Particles*, Academic Press, 1978.

[4] Deshpande, S. S., Anumolu, L. and Trujillo, M. F., Evaluating the Performance of the Two-Phase Flow Solver interFoam, *Computational Science and Discovery*,**5**, 2012, 014016.

[5] Garner, F.H., and Skelland, A.H.P., Some factors affecting droplet behaviour in liquid-liquid systems *Chemical Engineering Science*,**4**, 1955, 149–158.

[6] Lekhlifi, A., Antoni, M. and Ouazzani, J., Numerical Simulation of the Unsteady Hydrodynamics of a Water Droplet in Paraffin Oil, *Colloids and Surfaces A: Physicochemical and Engineering Aspects*,**365**, 2010, 70–78.

[7] Liu, Z., Hwang, S. S. and Reitz, R. D., Breakup Mechanisms and Drag Coefficients of High-Speed Vaporizing Liquid Drops, *Atomization and Sprays*,**6**, 1996, 353–376.

[8] Megaridis, C. M., Hodges, J. T., Xin, J., Day, J. M. and Presser, C., Internal Droplet Circulation Induced by Surface-Driven Rotation, *International Journal of Heat and Fluid Flow*,**15**, 1994, 364–377.

[9] Prakash, S. and Sirignano, W.A., Theory of Convective Droplet Vaporization with Unsteady Heat Transfer in the Circulating Liquid Phase, *International Journal of Heat and Mass Transfer*,**23**, 1980, 253–268.

[10] Qu, Q., Ma, P., Liu, P., Li, S. and Agarwal, R. K., Numerical Study of Transient Deformation and Drag Characteristics of a Decelerating Droplet, *AIAA Journal*,**54**, 2016, 490–505.

[11] Spells, K. E., A Study of Circulation Patterns Within Liquid Drops Moving Through a Liquid, *Proceedings of the Physical Society. Section B*,**65**, 1952, 541–546.

[12] Wadhwa, A. R., Magi, V. and Abraham, J., Transient Deformation and Drag of Decelerating Drops In Axisymmetric Flows, *Physics of Fluids*,**19**, 2007, 113301.

[13] Wang, X., Liu, G., Wang, K. and Luo, G., Measurement of Internal Flow Field During Droplet Formation Process Accompanied with Mass Transfer, *Microfluidics and Nanofluidics*,**19**, 2015, 757–766.